

# FPGA-Based Implementation of MPPT-Controller for PV Systems Under Partial Shading Conditions

Van Quang Binh NGO<sup>1</sup>, Kim Anh NGUYEN<sup>2</sup>, Khanh Quang NGUYEN<sup>2\*</sup>

<sup>1</sup> Faculty of Physics, University of Education, Hue University, 34 Le Loi, Hue, 530000, Vietnam  
nvqbinh@hueuni.edu.vn

<sup>2</sup> Faculty of Electrical Engineering, The University of Danang - University of Science and Technology, 54 Nguyen Luong Bang, Da Nang, 550000, Vietnam  
nkanh@dut.udn.vn, nkquang@dut.udn.vn (\*Corresponding Author)

**Abstract:** This paper presents the design and implementation of a FPGA-based Maximum Power Point Tracking (MPPT) controller using the Particle Swarm Optimization (PSO) algorithm for photovoltaic (PV) systems operating under partial shading conditions (PSC). The challenge in such conditions lies in accurately identifying the Global Maximum Power Point (GMPP), as the power-voltage (P-V) curve exhibits multiple local maximum power points (LMPPs). The traditional MPPT algorithms like the Perturb and Observe (P&O) and the Incremental Conductance (InC) algorithms often struggle to track the GMPP accurately in such complex scenarios. The proposed system takes advantage of the fact that the FPGA platform enables parallel processing to provide a real-time, high accuracy tracking of the GMPP. The simulation and experimental results confirm that the PSO-based MPPT controller significantly improves the GMPP tracking accuracy in comparison with the traditional methods. Although the PSO algorithm may feature slightly longer tracking times, its ability to accurately locate the GMPP in dynamic shading conditions ensures an optimal energy harvesting. This work emphasizes the practical benefits of implementing MPPT on a FPGA platform, offering a reliable solution for optimizing the performance of a PV system under varying solar radiation levels, thus improving the system's overall energy efficiency.

**Keywords:** FPGA, MPPT, PSO, PV System, PSC.

## 1. Introduction

The rising demand for sustainable energy has positioned PV systems as a crucial technology for generating clean electricity from solar energy. Despite their advantages, PV systems often face challenges in achieving an optimal efficiency due to environmental factors such as fluctuating sunlight intensity, temperature variations, and partial shading conditions (PSC) (Mohanty et al., 2019; Alshareef, 2022; Li et al., 2019). Under PSC, certain PV modules receive less irradiance, resulting in multiple LMPPs alongside a single GMPP on the P-V curve. Accurately tracking the GMPP is essential for maximizing energy harvesting, yet traditional MPPT algorithms often fall short under such conditions (Xia et al., 2024; Lv et al., 2024; Mihai et al., 2024).

Traditional MPPT techniques, including P&O and InC, struggle with the non-linear and multi-peak characteristics of P-V curves under PSC. Mohanty et al. (2016) addressed this limitation by introducing the Grey Wolf Optimization (GWO) technique, demonstrating an improved tracking accuracy and robustness compared to P&O. Similarly, Renaudineau et al. (2015) developed a PSO-based global MPPT algorithm, highlighting its ability to navigate complex search spaces and locate the GMPP effectively. These studies underscore the potential of metaheuristic algorithms for overcoming the limitations of traditional methods.

Building on these advancements, hybrid approaches have gained attention due to their enhanced performance (Akopov, 2024). Alshareef (2022) combined PSO with the Bat Algorithm (PSO-BA), achieving a superior tracking accuracy under PSC. Pal & Mukherjee (2020) performed a comparative analysis of various metaheuristic algorithms, showing that hybrid methods improve the convergence rates and tracking precision under dynamic shading conditions. Furthermore, Li et al. (2019) proposed a distributed PSO algorithm, which reduced oscillations and improved system stability.

Artificial intelligence (AI)-based methods have also emerged as promising solutions for MPPT. Ibelouad et al. (2021) utilized a multi-layer neural network to predict the optimal power output of PV systems under PSC, demonstrating the advantages of AI-driven approaches in managing complex conditions. Meanwhile, Al-Wesabi et al. (2024) and Xia et al. (2024) explored fuzzy logic and Ant Colony Optimization (ACO) hybrids, which showed an improved tracking speed and robustness under PSC. While algorithmic improvements are crucial, hardware implementation plays an equally important role in achieving these advances. Field Programmable Gate Arrays (FPGAs) have gained prominence for their ability to implement computationally intensive MPPT algorithms

efficiently (Kaced et al., 2017; Senthilvel et al., 2020; De Lima & Oliveira, 2024). Kaced et al. (2017) successfully demonstrated the feasibility of FPGA-based PSO-MPPT systems, achieving faster response times and reduced power losses in comparison with digital signal processors (DSPs). Similarly, Ricco et al. (2017) implemented a dual Kalman filter on FPGA, emphasizing the capability of the platform for real-time processing with high precision. De Lima & Oliveira (2024) further demonstrated the FPGA potential by implementing a fuzzy logic controller, showcasing its effectiveness under uneven shading. Despite these advancements, the integration of advanced MPPT algorithms like PSO into FPGA systems still requires further investigation to enhance real-time tracking accuracy, to preserve chip resources, and improve adaptability.

FPGA platforms enable parallel processing, ensuring an efficient GMPP tracking even in large systems with thousands of modules. This scalability allows the PSO-based algorithm to handle complex, multi-peak scenarios while minimizing hardware resource usage. Furthermore, FPGA's flexibility makes it well-suited for integrating large-scale PV systems into the existing grids, optimizing energy distribution, and improving grid stability. This approach enhances the feasibility of deploying advanced MPPT algorithms in real-world, large-scale applications (Orfanoudakis et al., 2024). This work addresses this gap by proposing a FPGA-based MPPT controller utilizing the PSO algorithm, specifically designed for PV systems operating under PSC.

The adoption of efficient design techniques, such as finite state machines (FSM), further minimizes hardware resource utilization, while implementing algorithms in Very High-Speed Hardware Description Language (VHDL) ensures precision and hardware efficiency (Boussaada et al., 2023; Kung et al., 2009; Ngo et al., 2024). Both the simulations and experiments carried out demonstrate the effectiveness of the system, emphasizing its capability to improve energy efficiency and reliability in dynamic environments.

The contribution of this study is the successful implementation of the PSO algorithm on a FPGA platform, illustrating its practical application for real-time MPPT in complex conditions. This integration not only demonstrates the feasibility of

deploying advanced algorithms on FPGA but also establishes a robust framework for future energy optimization systems, with the added benefits of resource conservation and design efficiency.

The remainder of this paper is organized as follows. Section 2 discusses the challenges of PV systems under partial shading conditions and the limitations of traditional MPPT techniques. Section 3 covers the design and implementation of the FPGA-based MPPT controller using the PSO algorithm, highlighting the system architecture. Further on, Section 4 presents the simulation and experimental results, obtained by comparing the PSO algorithm with traditional methods. Section 5 addresses the computational complexity and resource usage of the PSO algorithm on FPGA. Finally, Section 6 concludes this paper, outlining its practical implications and possible future research directions for enhancing the performance of a PV system.

## 2. Characteristics of the PV Array Under Partial Shading Conditions

Under PSC, PV panels behave differently than under normal conditions. Instead of generating electricity, they act as loads, which can cause "hot spots" that may damage the entire module. To mitigate this, PV panels are often equipped with parallel connected bypass diodes. This design allows current to bypass shaded sections, minimizing their impact on system performance. As a result, the P-V characteristic of the PV array typically features multiple LMPPs and a single GMPP. In this study, a simulation was conducted on a PV array with four modules connected in series to evaluate the MPPT algorithm based on PSO, as detailed in Table 1.

**Table 1.** TP250MBZ module specifications

Parameters	Value
Maximum Power ( $P_{\max}$ )	249 (W)
Voltage at $P_{\max}$ ( $V_{MPP}$ )	30 (V)
Current at $P_{\max}$ ( $I_{MPP}$ )	8.3 (A)
Open circuit voltage ( $V_{oc}$ )	36.8 (V)
Short circuit current ( $I_{sc}$ )	6.83 (A)

Three distinct cases with different solar radiation levels were considered, as shown in Figure 1. Case I features a baseline scenario, with uniform radiation applied across all panels. Case II involves a partial shading of panel 4, with the

remaining radiation limited to 500 W/m<sup>2</sup>. Case III involves a partial shading of panels 3 and 4, with radiation levels of 500 W/m<sup>2</sup> and 800 W/m<sup>2</sup>, respectively. Matlab/Simulink was employed to simulate the I-V and P-V curves for all scenarios, and the results are illustrated in Figures 2 and 3. In Case I, where no shading occurs, the PV array experiences uniform radiation, resulting in a single maximum on the PV curve characteristic. For Case II, partial shading on panel 4 causes two distinct MPPs to appear. Finally, in Case III, with varying radiation levels, three MPPs are observed, indicating the complexity of the shading effects on the performance of the PV system. From these cases, it is evident that the number of MPPs and their peak values can vary significantly depending on the shading conditions. Therefore, the correct identification of the GMPP under PSCs is vital for optimizing the efficiency of PV systems.

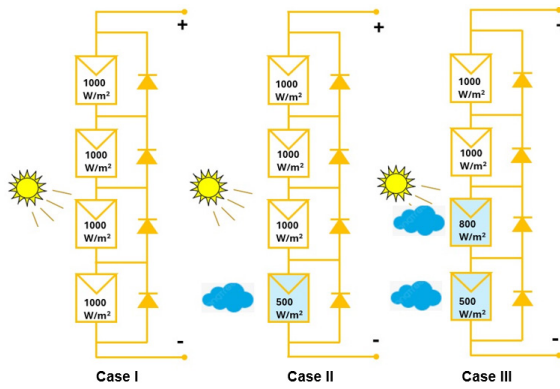


**Figure 1.** Various configurations of the PV array: case (I) uniform irradiance; case (II) PSC1 and case (III) PSC2

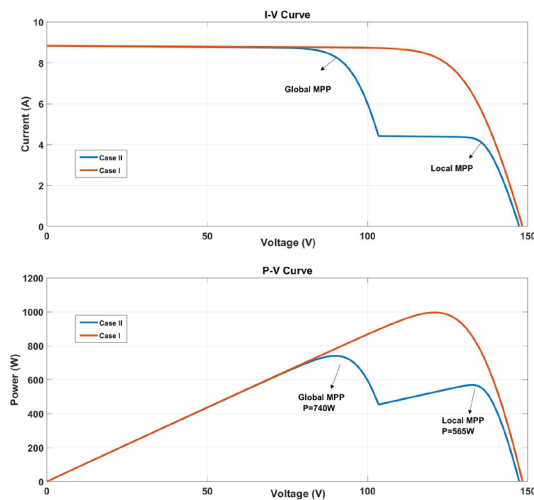


**Figure 2.** The P-V and I-V curves under uniform irradiance (Case I) and PSC1 (Case II)

### 3. FPGA-based MPPT Controller Design and Implementation

#### 3.1 The PSO-based MPPT Controller Design

The optimization process focuses on adjusting the PWM duty cycle, with the control being carried out through the MPPT algorithm. Initially, three particles are defined, each representing a different duty cycle. The optimization aims to enhance power generation from the PV panel, using this as the objective function. The duty cycles for each iteration are calculated using the following equation:

$$v_i^{k+1} = \omega v_i^k + c_1 r_1 (Pbest_i - D_i^k) + c_2 r_2 (Gbest_i - D_i^k), \quad (1)$$

$$D_i^k = D_i^{k+1} + v_i^k, \quad (2)$$

where  $v_i^{k+1}$  is the new velocity of particle  $i$  at the iteration  $k+1$ , and  $v_i^k$  is its current velocity at iteration  $k$ ,  $\omega$  is the inertia weight that balances exploration and exploitation,  $c_1$  and  $c_2$  are acceleration coefficients that determine the influence of the personal best and global best positions, respectively,  $r_1$  and  $r_1$  are random values between 0 and 1 used to introduce the stochastic behavior,  $Pbest_i$  is the best previous position (i.e. best duty cycle) found by particle  $i$ ,  $Gbest_i$  is the best global position found among all particles, and  $D_i^k$  is the current position (duty cycle) of particle  $i$  at the iteration  $k$ .

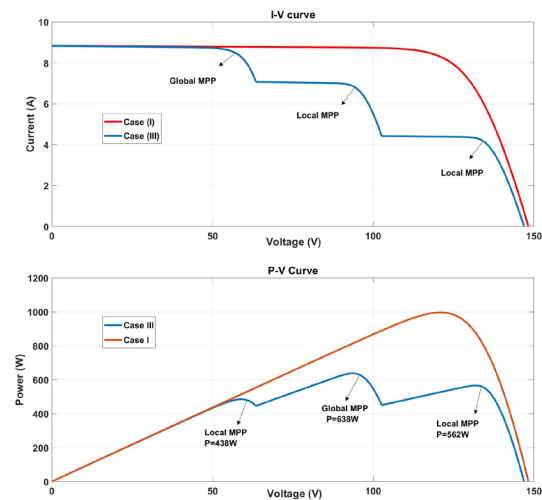


**Figure 3.** The P-V and I-V curves under uniform irradiance (case I) and PSC2 (case III)

The optimization process continues until the convergence criterion is met. Additionally, two extra conditions are applied to ensure a proper convergence. The proposed PSO-based MPPT method terminates and provides the global best solution if either the maximum number of iterations is reached or all particle velocities fall below a predefined threshold, as specified by the condition in equation (3):

$$|D_i^{k+1} - D_j^{k+1}| \leq \Delta D \quad (3)$$

The PSO algorithms generally focus on optimization problems with a fixed optimal solution. However, in this case, the fitness value representing the GMPP can change due to varying environmental conditions and load states. To effectively search for the new GMPP under these changing conditions, the particles are reinitialized whenever significant changes in insolation or shading patterns are detected by using equation (4):

$$\frac{|P_{PV,new} - P_{PV,old}|}{P_{PV,old}} \geq \Delta P(\%) \quad (4)$$

The proposed PSO algorithm is designed as follows:

*Step 1:* The initial values for parameters such as  $\omega$ , and  $c_1, c_2$  as well as  $r_1, r_2$  are set. The particle's position is defined to represent the converter duty cycle, with the fitness function determined by the output power. Randomly initialize the positions ( $D_i$ ) and velocities ( $V_i$ ) of the particles within the search space.

*Step 2:* The fitness of individual particles is accessed based on its current position (duty cycle  $D_i$ ) and the resulting output power.

*Step 3:* The  $P_{best}$  and  $G_{best}$  of each particle are identified by comparing the fitness values.

*Step 4:* The updates for each particle's velocity and position are calculated based on the formulas outlined in equations (1) and (2).

*Step 5:* The procedure concludes once the optimal solution is identified, or when the maximum number of iterations is reached. Otherwise, Steps 2–5 are repeated until convergence.

*Step 6:* If environmental conditions, such as shading or irradiance changes, significantly affect the PV system's performance, the algorithm is reinitialized to search for a new MPP.

### 3.2 FPGA Architecture

Figure 4 shows the implementation of the proposed MPPT controller for the PV system using FPGA. The control architecture system consists of several components: an analog to-digital converter (ADC) for signal read-in and conversion, a frequency divider, and the PSO-based MPPT controller and tested via simulation in ModelSim to evaluate their performance before deploying them on the Altera MAX 10 FPGA. The MPPT system operates at a sampling frequency of 25 kHz. Operating at a clock rate of 50 MHz, the FPGA controller utilizes a frequency divider to generate clock signals of 50 MHz (CLK), 25 MHz (CLK-STEP), and 25 kHz (CLKPWM), powering all circuits within the system-on-chip.

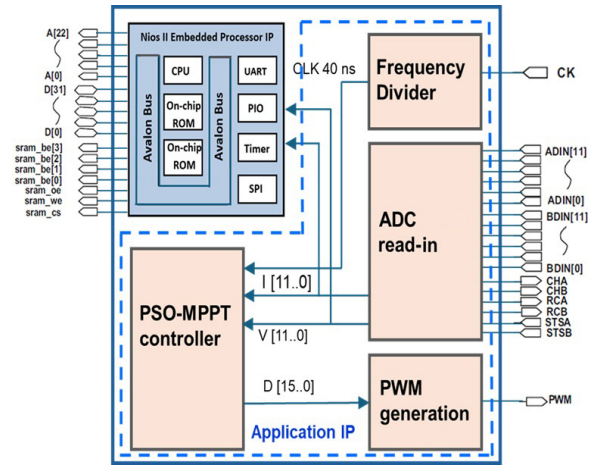


Figure 4. FPGA-based architecture of the PSO-MPPT controller

### 3.3 Algorithm Implementation

Figure 5 shows the application of a FSM technique to model the control algorithm of the MPPT system that uses PSO. In this diagram, the data format is 16-bit with Q15 representation and 2's complement arithmetic operations. Although the PSO algorithm is complex, the FSM successfully integrates the control framework and can be efficiently implemented in VHDL. The multiplier and adder are designed according to the Altera Library Parameterized Modules standard. The FSM operates through 17 sequential steps to perform the required computations. Steps  $S_0 - S_8$  are responsible for calculating the individual positions and evaluating the objective function, in steps  $S_9 - S_{15}$  the particle velocities and their respective positions are updated, and in step  $S_{16}$  the termination condition is evaluated, and the

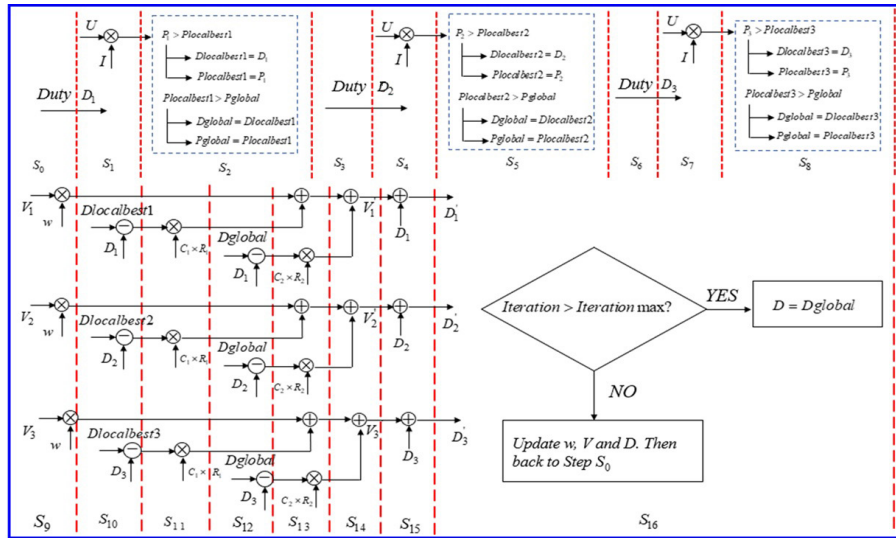


Figure 5. FSM diagram of the PSO-MPPT algorithm

duty cycle is output. Each step can be completed in 40 ns (at a clock frequency of 25 MHz), so the total time for executing the 17 steps is 0.68  $\mu$ s. Lastly, the PSO and PWM modules utilize 2,368 Logic Elements (LEs) and 71,650 RAM bits on the FPGA MAX 10 10M50DAF484C7G.

### 3.4 Computational Complexity and Resource Consumption

The computational cost of the PSO algorithm is significantly higher than that of the P&O algorithm. Specifically, PSO requires 15 multiplications, 9 additions, and 6 subtractions, while P&O only needs 3 multiplications, 2 additions, and 6 subtractions. This complexity arises from the iterative calculation of particle positions and velocities in the search space to find the GMPP. PSO uses 12,396 logic elements (25% of the chip’s resources) and 150,346 memory bits (9% of the memory). While the resource demands are higher in comparison with P&O (which uses 18% of the chip’s resources, and 6% of the memory), they remain optimized for modern chips as the total resource usage is still relatively small. Despite an increased resource consumption, PSO offers significant advantages, especially in complex partial shading conditions and multi-peak scenarios where traditional methods like P&O fail to achieve an optimal performance. The FSM design method allows one to save a substantial amount of chip resources, optimizing resource usage by minimizing unnecessary logic elements. Therefore, although PSO requires more resources than the traditional methods, its ability to handle challenging conditions and achieve a superior

performance justifies additional resource usage, making it an effective and optimized solution for real-world applications.

### 4. ModelSim/Simulink Co-Simulation and its Results

To validate the performance of the proposed MPPT controller architecture for a standalone PV system, both simulations and experiments are presented in this section and in Section 5. The simulation setup, as shown in Figure 6, utilizes the SimPowerSystem blockset in Simulink to model the PV panels, and the DC/DC converter, and the interface with the EDA simulator in ModelSim for co-simulation with the VHDL code for implementing the PSOMPPT algorithm. The PV module specifications in this section are consistent with those outlined in Section 2, and the validation scenarios (Case I, Case II, and Case III) are used for the simulation.

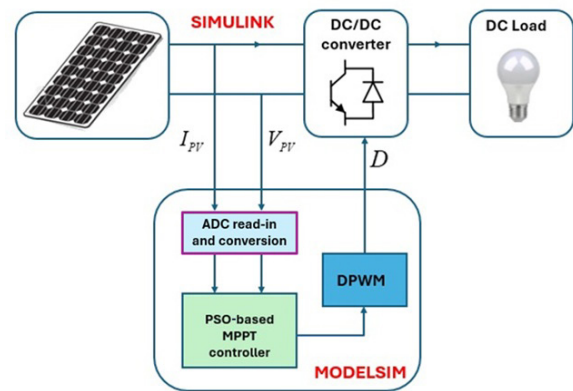


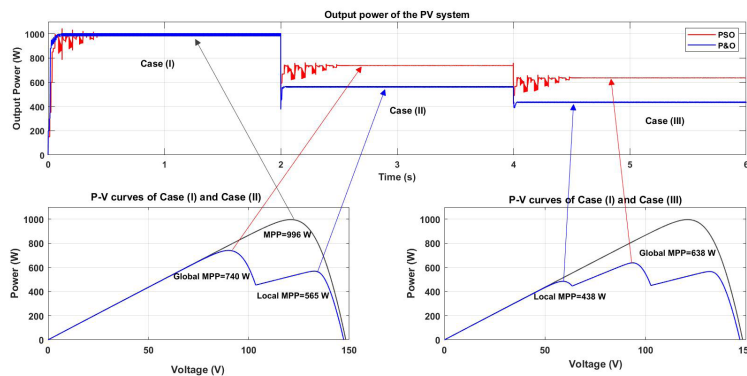
Figure 6. Modelsim/Simulink co-simulation

Figure 7 displays the simulation results for comparing the performance of the PSO and P&O MPPT algorithms under three scenarios: Case I (uniform radiation), Case II (partial shading on one panel), and Case III (partial shading on two panels). In Case I, with all panels exposed to uniform radiation ( $1000 \text{ W/m}^2$ ), both algorithms track the single MPP successfully, maintaining a stable output power of 996 W, as shown by the P-V curve. This indicates that both algorithms perform equally well under ideal conditions. In Case II, with Panel 4 partially shaded and receiving only  $500 \text{ W/m}^2$  of radiation, the P-V curve exhibits two peaks: a GMPP at 740 W and a LMPP at 565 W. The PSO algorithm accurately identifies the GMPP, ensuring an optimal power output, while the P&O algorithm gets stuck at the LMPP, resulting in a lower power output. In Case III, where Panels 3 and 4 experience partial shading ( $800 \text{ W/m}^2$  and  $500 \text{ W/m}^2$ , respectively), the P-V curve exhibits an increased complexity, showing three distinct peaks. The PSO algorithm identifies the GMPP at 638 W, while the P&O algorithm locks onto a lower local peak at 438W, leading to a suboptimal performance. Although the PSO algorithm performs well in multi-peak situations and effectively identifies the GMPP, it has the disadvantage of slower tracking in comparison with the P&O algorithm.

The PSO's tracking time is 0.29 seconds, which is 0.2 seconds longer than that of P&O. This delay is due to the iterative process required by PSO, as it updates multiple particles within the search space to find the optimal solution. However, this trade-off is acceptable considering PSO's superior performance in optimizing the PV system output under complex PSC, where simpler algorithms like P&O struggle to perform effectively.

## 5. Experimental System and Results

After confirming the correctness of VHDL code of the proposed MPPT controller through simulation, the code was implemented directly on the experimental FPGA-based MPPT controller for the PV system. Figure 8 shows the experimental setup, which consists of key components such as a PV module, a FPGA board featuring an Altera MAX10 FPGA, a MOSFET driver, a boost converter, and sensors for monitoring current and voltage. The PV module used in the study is the WorldEnergy 60W, with the following specifications:  $P_{\max} = 60 \text{ W}$ , a voltage (at  $P_{\max}$ )  $V_{MPP} = 18$ , a current  $I_{MPP} = 3.33 \text{ A}$  (at  $P_{\max}$ ). The open circuit voltage  $V_{OC} = 21.06 \text{ V}$ , while the short circuit current  $I_{SC} = 3.89 \text{ A}$ , and the boost converter is configured with the following parameters: inductance  $L = 1 \text{ mH}$ , capacitance



**Figure 7.** Power curve for the PV array during the simulation of dynamic PSC for the PSO and P&O algorithms

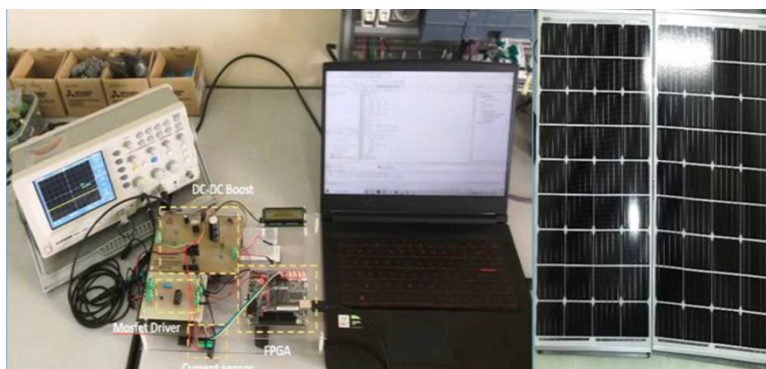


**Figure 8.** The experimental system

$C_1 = 440F$ , capacitance  $C_2 = 33F$ , and a switching frequency of 25 kHz.

The experiment utilizes two different partial shading patterns, and the corresponding P-V curve features are displayed in Figure 9. These curves are generated by a scanning procedure where the duty cycle progressively increases from 0 to 1 over the span of one second, following the approach that Kaced et al. (2017) implemented in their study. In the first shading pattern, the P-V curve reveals two MPPs: a LMPP at 31.2 W and a GMPP at 38.8 W, indicating the peak power outputs under this condition. In the second shading pattern, the curve becomes more intricate, showing three peaks: LMPP1 at 14.2 W, GMPP at 36.9W, and LMPP2 at

22.9W. The GMPP is located at 16.8 V, underlining the importance of precise tracking for an optimal system performance. These findings demonstrate the complexities induced by partial shading, where multiple peaks make GMPP identification challenging, necessitating the use of advanced MPPT algorithms to optimize energy harvesting. The results shown in Figure 10 (a, b) validate the effectiveness of the PSO-MPPT method, implemented on a FPGA, for tracking the GMPP. In the first scenario, the PSO algorithm accurately follows the GMPP, keeping the operating point  $V = 17.5V$  and  $I = 2.2A$ . In the second scenario, the operating point remains around 16.8 V and 2.17 A. These findings confirm the reliability of the PSO algorithm in both scenarios.

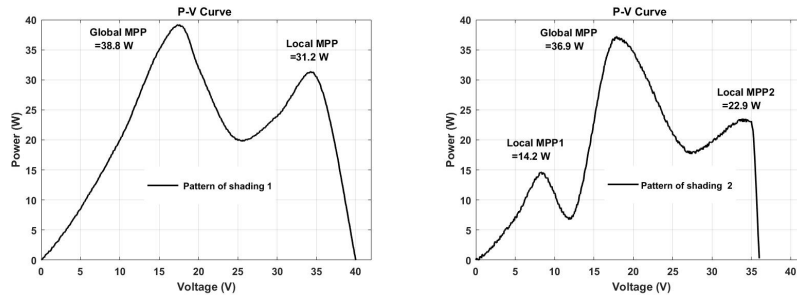
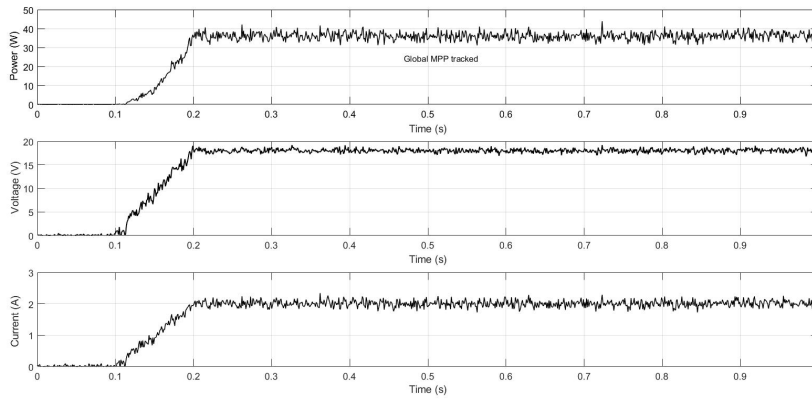
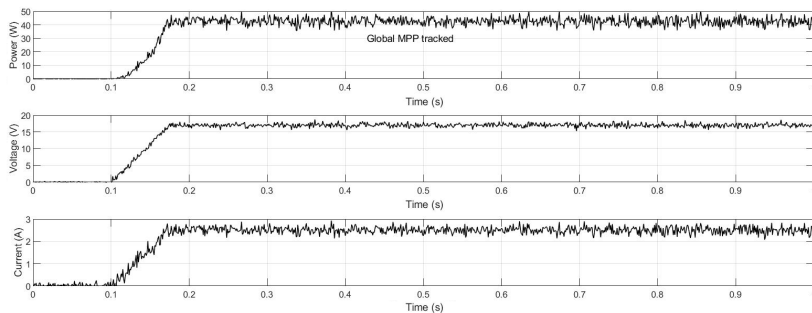


Figure 9. P-V curve measurements under two different PSCs



(a) Pattern of shading 1



(b) Pattern of shading 2

Figure 10. Measured PV power, voltage and current waveforms

## 6. Conclusion

This study successfully demonstrates the implementation of an FPGA-based MPPT controller using the PSO algorithm for PV systems operating under PSC. The proposed system utilizes the computational strengths of FPGA to provide the real-time tracking of the GMPP with high accuracy in complex multipeak P-V curves. Both the simulation and experiments confirm the effectiveness of the PSO technique, highlighting its superior performance in comparison with the traditional MPPT method P&O. Although the PSO controller exhibits slightly longer tracking times,

this is balanced by its reliable ability to accurately identify the GMPP, even under dynamic shading conditions, ensuring an optimal energy harvesting. The FPGA-based PSO solution offers a robust and flexible approach to optimizing the PV system's performance, particularly in environments with fluctuating solar radiation, and holds significant potential for an efficient energy harvesting in modern photovoltaic applications.

## Acknowledgements

This research is funded by Hue University under grant number DHH2025-03-206.

## REFERENCES

- Akopov, A. S. (2024) A Clustering-Based Hybrid Particle Swarm Optimization Algorithm for Solving a Multisectoral Agent-Based Model. *Studies in Informatics and Control*. 33(2), 83-95. <https://doi.org/10.24846/v33i2y202408>.
- Alshareef, M. (2022) A New Particle Swarm Optimization with Bat Algorithm Parameter-Based MPPT for Photovoltaic Systems under Partial Shading Conditions. *Studies in Informatics and Control*. 31(4), 53-66. <https://doi.org/10.24846/v31i4y202206>.
- Al-Wesabi, I., Farh, H. M. H., Fang, Z. et al. (2024) A comprehensive comparison of advanced metaheuristic photovoltaic maximum power tracking algorithms during dynamic and static environmental conditions. *Heliyon*. 10(18), 1-24. <https://doi.org/10.1016/j.heliyon.2024.e37458>.
- Boussaada, M., Abdelati, R., Lahdhiri, H. et al. (2023) PV Characterization and MPPT Based on Characteristic Impedance Using Arduino Board and MATLAB Interface. *Studies in Informatics and Control*. 32(1), 91-100. <https://doi.org/10.24846/v32i1y202309>.
- De Lima, T. M. & Oliveira, J. A. C. B. (2024) FPGA-Based Fuzzy Logic Controllers Applied to the MPPT of PV Panels - A Systematic Review. *IEEE Transactions on Fuzzy Systems*. 32(8), 4260-4269. <https://doi.org/10.1109/TFUZZ.2024.3392846>.
- Ibnelouad, A., El Kari, A., Ayad, H. et al. (2021) Multilayer Artificial Approach for Estimating Optimal Solar PV System Power Using the MPPT Technique. *Studies in Informatics and Control*. 30(4), 109-120. <https://doi.org/10.24846/v30i4y202110>.
- Kaced, K., Larbes, C., Ait-Chikh, S. M. et al. (2017) FPGA implementation of PSO based MPPT for PV systems under partial shading conditions. In: *6th International Conference on Systems and Control (ICSC), 7-9 May 2017, Batna, Algeria*. Piscataway, NJ, USA, IEEE. pp. 150-155.
- Kung Y. S., Quang N. K. & Van Anh L. T. (2009) FPGA-based neural fuzzy controller design for PMLSM drive. In: *2009 International Conference on Power Electronics and Drive Systems (PEDS), Taipei, Taiwan*. Piscataway, NJ, USA, IEEE. pp. 222-227.
- Li, H., Yang, D., Su, W. et al. (2019) An Overall Distribution Particle Swarm Optimization MPPT Algorithm for Photovoltaic System Under Partial Shading. *IEEE Transactions on Industrial Electronics*. 66(1), 265-275. <https://doi.org/10.1109/TIE.2018.2829668>.
- Lv, R., Zhu, Y. & Yang, Y. (2024) Robust Design of Perturb & Observe Maximum Power Point Tracking for Photovoltaic Systems. *IEEE Transactions on Industry Applications*. 60(4), 6547-6558. <https://doi.org/10.1109/TIA.2024.3397971>.
- Mihai, L., Olteanu, S. C. & Popescu, D. (2024) Trajectory Optimisation for Photovoltaic Panels with 2 Degrees of Freedom. *Studies in Informatics and Control*. 33(4), 25-35 <https://doi.org/10.24846/v33i4y202403>.
- Mohanty, S., Subudhi, B. & Ray, P. K. (2016) A New MPPT Design Using Grey Wolf Optimization Technique for Photovoltaic System Under Partial Shading Conditions. *IEEE Transactions on Sustainable Energy*. 7(1), 181-188. <https://doi.org/10.1109/TSTE.2015.2482120>.
- Ngo, V. Q. B., Kim Anh N. & Khanh Quang N. (2024) FPGA-Based Adaptive PID Controller Using MLP Neural Network for Tracking Motion Systems. *IEEE Access*. 12, 91568-91574. <https://doi.org/10.1109/ACCESS.2024.3422015>.

- Orfanoudakis, G. I., Lioudakis, E., Foteinopoulos, G. et al. (2024) Dynamic Global Maximum Power Point Tracking for Partially Shaded PV Arrays in Grid-Connected PV Systems. *IEEE Journal of Emerging and Selected Topics in Industrial Electronics*. 5(4), 1481-1492. <https://doi.org/10.1109/JESTIE.2024.3389686>.
- Pal, R. S. & Mukherjee, V. (2020) Metaheuristic based comparative MPPT methods for photovoltaic technology under partial shading condition. *Energy*. 212, art. no. 118592. <https://doi.org/10.1016/j.energy.2020.118592>.
- Renaudineau, H., Donatantonio, F., Fontchastagner, J. et al. (2015) A PSO-Based Global MPPT Technique for Distributed PV Power Generation. *IEEE Transactions on Industrial Electronics*. 62(2), 1047-1058. <https://doi.org/10.1109/TIE.2014.2336600>.
- Ricco, M., Manganiello, P., Monmasson, E. et al. (2017) FPGA-Based Implementation of Dual Kalman Filter for PV MPPT Applications. *IEEE Transactions on Industrial Informatics*. 13(1), 176-185. <https://doi.org/10.1109/TII.2015.2462313>.
- Senthilvel, A., Vijeyakumar, K.N. & Vinothkumar, B. (2020) FPGA based implementation of MPPT algorithms for photovoltaic system under partial shading conditions. *Microprocessors and Microsystems*. 77, art. no. 103011. <https://doi.org/10.1016/j.micpro.2020.103011>.
- Xia, K., Li, Y. & Zhu, B. (2024) Improved Photovoltaic MPPT Algorithm Based on Ant Colony Optimization and Fuzzy Logic Under Conditions of Partial Shading. *IEEE Access*. 12, 44817-44825. <https://doi.org/10.1109/ACCESS.2024.3381345>.



This is an open access article distributed under the terms and conditions of the Creative Commons Attribution-NonCommercial 4.0 International License.